Biosaintifika 16 (3) (2024): 437- 448 p-ISSN 2085-191X | e-ISSN 2338-7610
Journal of Biology & Biology Education https://journal.unnes.ac.id/nju/index.php/biosaintifika

Gold Nanoparticles of *Lactobacillus kimchicus* DCY51^T Suppressed Lipopolysaccharide-Stimulated Inflammatory Reactions in RAW264.7 Macrophage Cells

Johan Sukweenadhi[1,2*], Yaxi Han[3], Dae-Hyo Jung[3], Josua Markus[3], Yeon-Ju Kim[2,3], Se-Chan Kang[2,3]

[1]University of Surabaya, Faculty of Biotechnology, Department of Plant Biotechnology, Surabaya 60293, East Java, Republic of Indonesia
[2]Center of Excellence for Food Products and Health Supplements for Degenerative Conditions, University of Surabaya, Surabaya 60293, East Java, Republic of Indonesia
[3]Kyung Hee University, College of Life Science, Department of Oriental Medicinal Biotechnology, Yongin-si, Gyeonggi-do 17104, Republic of South Korea

*Corresponding author: sukwee@staff.ubaya.ac.id

Submitted: 2024-06-24. Revised: 2024-09-18. Accepted: 2024-11-22.

Abstract. Excessive inflammation can lead to chronic diseases, necessitating the development of effective anti-inflammatory therapies. This study investigates the anti-inflammatory effects of gold nanoparticles (AuNps) synthesized using *Lactobacillus kimchicus* DCY51^T, a probiotic strain from Korean kimchi. The objective is to explore the potential of DCY51^T-AuNps in modulating inflammatory responses in RAW264.7 macrophage cells. Methods: AuNps were synthesized through a meticulous procedure involving the probiotic *Lactobacillus kimchicus* DCY51^T. The isolation and subsequent cultivation of the RAW264.7 macrophage cell line in the DMEM medium formed the basis for the research methodology. Results: Following the establishment of the cellular platform, the cells were treated with DCY51^T-AuNps, revealing a noteworthy reduction in the expression of key inflammatory mediators such as nitric oxide (NO), prostaglandin E2 (PGE2), interleukin-6 (IL-6), and tumor necrosis factor-α (TNF-α). A pivotal aspect of the study focused on the inhibitory effects of DCY51^T-AuNps on the lipopolysaccharide (LPS)-induced activation of the NF-κB/mitogen-activated protein kinase (MAPK) pathway within RAW264.7 cells. Conclusion: This inhibition was instrumental in modulating the inflammatory response, showcasing the potential therapeutic relevance of DCY51T-AuNps in combating inflammation. The novelty lies in using a probiotic-derived synthesis method, offering a sustainable and biocompatible approach to nanoparticle production. The benefit of this research not only underscores the anti-inflammatory prowess of DCY51^T-AuNps on RAW264.7 macrophages but also contributes to the broader scientific discourse on the biomedical applications of gold nanoparticles synthesized from probiotic sources, potentially benefiting the development of new anti-inflammatory therapies and advancing nanomedicine.

Keywords: anti-inflammatory; gold nanoparticles; green synthesis; mitogen-activated protein kinases; probiotics

How to Cite: Sukweenadhi, J., Han, Y., Jung, D.-H., Markus, J., Kim, Y.-J., & Kang, S.-C. (2024). Gold Nanoparticles of *Lactobacillus kimchicus* DCY51^T Suppressed Lipopolysaccharide-Stimulated Inflammatory Reactions in RAW264.7 Macrophage Cells. *Biosaintifika: Journal of Biology & Biology Education, 16(3)*, 437-448.

DOI: http://dx.doi.org/10.15294/biosaintifika.v16i3.17103

INTRODUCTION

Inflammation is an evolutionarily conserved host response to stress, tissue injury, and infection. This process involves modifications in tissue homeostasis and blood flow, as well as the activation and migration of immune cells, and the coordinated spatio-temporal release of cytokines and other mediators (Agarwal et al., 2019). Inflammation may serve as a beneficial response initiated by harmful stimuli and situations, including infection and tissue damage (Smale, 2010). Nevertheless, the conventional perception of inflammation solely as a response to injury or infection may need to widen to include inflammatory processes generated by several additional unfavorable situations (Medzhitov, 2008). Overstimulated macrophages might aggravate the symptoms of the inflammatory process (Ahn et al., 2015).

Numerous inflammatory signaling pathways are powerfully triggered by lipopolysaccharide (LPS) and it prompts macrophages to generate numerous inflammatory mediators (Su et al.,

2011). The transcription factor NF-κB has garnered attention in the context of inflammatory responses, primarily due to the way that different mediators and cytokines activate this transcription factor (Beinke & Ley, 2004). The primary subunits comprising the activated form of NF-κB are p50 and p65 (Hart et al., 1998). In inactive cells, NF-κB exists as a heterodimer in the cytosol, bound to an inhibitory protein called inhibitor-κB (Iκ-B). Upon stimulation by various inflammatory triggers like lipopolysaccharide (LPS), cytokines, oxidants, and viruses, the NF-κB heterodimer swiftly relocates to the nucleus. Once in the nucleus, it initiates the transcription of specific genes, including those responsible for pro-inflammatory cytokines, adhesion molecules, chemokines, and inducible enzymes such as inducible NO synthase (iNOS;Ahn et al., 2016; Gasparini & Feldmann, 2012; Rius-Pérez et al., 2020). Apart from NF-κB, the regulation of inflammatory mediator production relies on mitogen-activated protein kinases (MAPKs), which include extracellular signal-regulated kinase (ERK), c-Jun NH2-terminal kinase (JNK), and p38 (Ahn et al., 2016; Feng et al., 2011; Kyriakis & Avruch, 2012). The MAPKs form a group of protein-serine/threonine kinases that connect external signals to the mechanisms governing fundamental cellular processes, including cell proliferation, survival, death, and differentiation (Yang et al., 2013). Given the crucial involvement of NF-κB and MAPK in the reinforcing cycle of the inflammatory response, they have emerged as plausible targets for novel anti-inflammatory therapies (Liu et al., 2013; Wu et al., 2020).

Gold nanoparticles have garnered significant scientific and technological attention due to their straightforward synthesis, chemical stability, and distinctive optical characteristics (Alkilany & Murphy, 2010; Bansal et al., 2020; Fatimah et al., 2020; Pan et al., 2007). Green synthesis, mainly facilitated by plant extracts, is not only cost-effective but also advantageous (Huq et al., 2022; Sukweenadhi et al., 2021). Moreover, this approach is emerging as a pathway for creating a new category of probiotics-mediated and non-toxic carriers for targeted drug delivery systems, cancer diagnostics, photothermal therapy, biosensing, and medical imaging (Markus et al., 2016). Additionally, some studies suggest that gold nanoparticles (AuNps) exhibit anti-inflammatory effects by modulating inflammatory mediators and suppressing the MAPK and NF-κB signaling pathways in LPS-stimulated RAW264.7 cells (Ahn et al., 2018; Rehman et al., 2012).

In this current investigation, we explored the anti-inflammatory properties of aqueous suspensions containing DCY51^T-AuNps in RAW264.7 macrophages and unraveled the mechanism behind the anti-inflammatory effects induced by these suspensions. The decision to utilize this specific probiotic strain, derived from Korean kimchi, was strategic due to its distinctive attributes. The introduction of *Lactobacillus kimchicus* DCY51^T in the green synthesis of AuNps marks a novel and innovative approach. The selection of *Lactobacillus kimchicus* DCY51^T is grounded in its inherent capability to facilitate the bioreduction of HAuCl4 into AuNps through an intracellular membrane-bound mechanism. This unique characteristic of the bacteria ensures the creation of AuNps with favorable features, such as spherical shapes ranging from 5 to 30 nm. Furthermore, the resulting AuNps maintain an average crystallite size of 13 nm and exhibit sustained stability in both physiological buffer and biological media (Markus et al., 2016).

The research purposes extend beyond the mere synthesis of nanoparticles; they delve into the exploration of the anti-inflammatory effects of DCY51^T-AuNps by utilizing RAW264.7 macrophages. Beyond the simple manufacturing of nanoparticles, the purpose of this research is to further our knowledge of these gold nanoparticles' potential as a treatment for inflammation. We aim to gain a new understanding of DCY51T-AuNps' potential as anti-inflammatory medicines by examining the basic mechanisms by which they alter inflammatory responses. Given the increasing need for efficient treatments for chronic inflammatory illnesses, which represent huge global health burdens, this finding is especially important. By utilizing *Lactobacillus kimchicus* DCY51^T unique characteristics for AuNp production, we hope to further the fields of biotechnology and nanotechnology. Probiotic bacteria's creative application in nanoparticle synthesis not only improves our comprehension of biological processes but also creates new avenues for the ecologically responsible and sustainable manufacturing of nanomaterials. This strategy fits nicely with the growing need for environmentally friendly synthesis techniques that support sustainability.

These AuNps are used in a wide range of fields, including photothermal therapy, biosensing, targeted drug delivery systems, cancer diagnostics, and medical imaging. The produced nanoparticles' low cost and non-toxicity make

them useful instruments for tackling urgent issues in technology and healthcare. These nanoparticles could, for example, increase the accuracy and effectiveness of therapies in targeted medication delivery, lowering adverse effects and improving patient outcomes. The distinct characteristics of AuNps may result in more precise cancer diagnosis and efficient treatment alternatives. Our research efforts therefore aim to both broaden the boundaries of scientific understanding and convert these discoveries into workable solutions that have a constructive influence on society. Our goal is to enhance the quality of life for those with chronic inflammatory diseases by creating novel anti-inflammatory treatments. Additionally, DCY51^T-AuNps wider uses in a range of biomedical domains demonstrate their potential to transform established procedures and aid in the creation of novel healthcare solutions.

METHODS

Reagents and materials

Gibco-BRL provided Dulbecco with its modified Eagle's medium (DMEM) (Grand Island, NY, USA). Lipopolysaccharides (LPS), sodium nitrite ($NaNO_2$) solution, Dexamethasone, and Griess reagent were purchased from Sigma-Aldrich Co. (St. Louis, MO, USA). Anti-rabbit antibodies coupled with horseradish peroxidase (HRP) were obtained from R&D Systems (Minneapolis, MN, USA). Fetal bovine serum (FBS), phosphate-buffered saline (PBS), and penicillin-streptomycin (P/S) were acquired from WelGENE Inc. (Daegu, Korea). Santa Cruz Biotechnology provided the primary antibodies that were used to target NF-κB, JNK, ERK, phospho-JNK, phospho-ERK1/2, and β-actin (Santa Cruz, CA, USA). The DCY51^T-AuNps were obtained from a previous study, synthesized by *Lactobacillus kimchicus* DCY51^T, exhibiting a spherical shape with sizes ranging from 5 to 30 nm (Markus et al., 2016).

Cell culture

The RAW264.7 murine macrophage cell line was procured from the American Type Culture Collection and the Korean Cell Line Bank in Seoul, South Korea. 10% heat-inactivated fetal bovine serum (FBS) and 1% penicillin/streptomycin (P/S) were added to the DMEM medium (GIBCO-BRL, Rockville, MD) in order to support the cell culture (WelGENE Inc., Daegu, Korea). Incubation was carried out at 37°C in a humidified atmosphere containing 5% CO_2 (Ahn et al., 2018).

Cytotoxicity assay

The cytotoxicity assay involved the use of 3-(4, 5-dimethyl-2-thiazolyl)-2, 5-diphenyl-2H tetrazolium bromide (MTT), following the previous method (Ahn et al., 2015). RAW264.7 cells were exposed to varying concentrations (0 to 100 μg mL^{-1}) of DCY51^T-AuNps aqueous suspensions for 24 hours. Afterward, each well received 20 μL of MTT assay solution (5 mg mL^{-1}) and was left to incubate for 3 hours. Following incubation, by using a multi-mode plate reader (BioTek Instrument, Winooski, VT) at a test wavelength of 570 nm and a reference wavelength of 630 nm, the media was replaced with 100 μL of dimethyl sulfoxide (DMSO), and the formazan produced by live cells was quantified after 30 minutes of incubation. The cell viability was expressed as a percentage relative to the control (untreated cells).

Measurement of NO, TNF-α, PGE2 and IL-6

RAW264.7 cells underwent co-treatment with 1 μg mL^{-1} LPS and DCY51^T-AuNps aqueous suspensions, followed by a 24-hour incubation period. After incubation, the supernatant was collected for subsequent assays. Nitrite levels in the medium were determined using the Griess reagent. After mixing 100 μL of the culture supernatant with the same amount of Griess reagent, a microplate reader was used to measure the absorbance at 540 nm (Bio-Tek Instruments, Winooski, Inc.). Each experimental setup contained a typical sodium nitrite curve. Using enzyme-linked immunosorbent assay (ELISA) kits obtained from R&D Systems (Minneapolis, MN, USA), the levels of TNF-α, PGE2, and IL-6 were measured in accordance with the manufacturer's instructions (Wang et al., 2014).

Measurement of intracellular reactive oxygen species

To assess intracellular reactive oxygen species (ROS) levels following the previous method (Ahn, et al., 2016), 5 × 10^3 RAW264.7 cells were seeded in 24-well plates. After 24 hours, the cells were exposed to 1 μg mL^{-1} LPS with or without varying concentrations of DCY51^T-AuNps aqueous suspensions and were subsequently incubated for an additional 24 hours at 37°C in a 5% CO_2 incubator. Following the incubation period, the medium was removed, and the cells underwent three washes with PBS. After that, 10 μM 2',7'-Dichlorodihydrofluorescein

Diacetate (DCFH-DA) was applied to the cells and left them in the dark for 30 minutes. Next, a microplate reader (BioTek Instrument, Winooski, VT) with an excitation wavelength of 485 nm and an emission wavelength of 535 nm was used to measure the fluorescence generated by DCFH.

Reverse transcription polymerase chain reaction

In a six-well plate, RAW264.7 cells were plated at a density of 10^6 cells per well for the purpose of reverse transcription polymerase chain reaction (RT-PCR). Following a 24-hour incubation period, cells were subjected to a further 24-hour treatment, either in the presence or absence of LPS stimulation and with or without various concentrations of DCY51^T-AuNps aqueous suspensions. TRIzol reagent was used to isolate RNA (Sigma, St. Louis, MO). Using a cDNA synthesis kit (Thermo Scientific, EU, Lithuania) and the manufacturer's instructions, first-strand cDNA synthesis was performed. Quantitative real-time polymerase chain reaction (qRT-PCR) amplification was performed using an SYBR Green qPCR Super Mix UDG kit and an R-Corbett Rotor-Gene Model 6000 (Corbett Research, Sidney, Australia) with a total of 1 µL of the cDNA product as the template (Livak & Schmittgen, 2001).

Western blot analysis

Whole cell lysates were first subjected to separation using 10% sodium dodecyl sulfate–polyacrylamide gel electrophoresis (SDS–PAGE) and then transferred to a PVDF membrane for Western blot analysis. After blocking with 5% skim milk (w/v), the membranes were left to incubate overnight at 4°C with primary antibodies. Subsequently, following five washes with Tris-buffered saline-Tween (TBS-T) (1×), the membranes underwent exposure to goat anti-mouse or anti-rabbit IgG conjugated with horseradish peroxidase (HRP) for a duration of 2 hours at room temperature. The detection of immunolabeling was accomplished using enhanced chemiluminescence (Millipore Corporation, Billerica, MA), and the densitometry of bands was quantified using ImageJ software (Ahn et al., 2017).

Immunofluorescence staining

For immunofluorescence staining, RAW264.7 cells were cultured on 8-well culture slides (SPL Life Sciences Co., Ltd., Korea) overnight. The cells were pre-treated with DCY51^T-AuNps aqueous suspensions for 2 hours, followed by LPS (1 µg mL^{-1}) stimulation for an additional 2 hours. After washing thoroughly with PBS, the cells underwent fixation in 3.7% formaldehyde and permeabilization with 0.5% Triton X-100 for 10 minutes. After that, rabbit monoclonal anti-NF-κB p65 antibodies were added, and the cells were incubated for the entire night at 4°C (1:200, Santa Cruz Biotechnology, Santa Cruz, CA, USA). Once the slides were cleaned, they were left in the dark for one hour and exposed to Alexa Fluor1488 goat anti-rabbit IgG (1:200; Cell Signaling Technology, Beverly, MA, USA). 4'-6-diamidino-2-phenylindole (DAPI, 10 mg mL-1) was used to stain nuclei for ten to fifteen minutes. An inverted research fluorescence microscope was used to take pictures of the cells (Ahn et al., 2017).

Statistical analysis

A statistical analysis was performed utilizing the software GraphPad 6.04. (La Jolla, CA). The findings are shown as mean ± SEM. The two-way analysis of variance (ANOVA) and student's t-test were used to assess the statistical significance of the variations in values between the treated and untreated groups. When $p < 0.05$, differences were deemed significant.

Table 1. The list of primer sequence

Primer Name	Primer Sequence
COX-2	F: 5'- GGATGCGCTGAAACGTGGA -3' R: 5'- CAGGAATGAGTACACGAAGCC -3'
IL-6	F: 5'- CCGGAGAGGAGACTTCACAG -3' R: 5'- GGAAATTGGGGTAGG AAG GA -3'
TNF-α	F: 5'- AGTCCGGGCAGGTCTACTTT -3' R: 5'- GCACCTCAGGGAAGAGTCTG -3'
iNOS	F: 5'- GTGGTGACAACGACATTTGG -3' R: 5'- GGCTGGACTTTTCACTCTGC -3'
GAPDH	F: 5'- CAAGGTCATCCATGACAACTTTG -3' R: 5'- GTCCACCACCCTGTTGCTGTAG -3'

RESULTS AND DISCUSSION

Effects of DCY51^T-AuNps aqueous suspensions on the viability of RAW264.7 cells and intracellular ROS production

The impact of DCY51^T-AuNps aqueous suspensions on the viability of RAW264.7 cells was assessed through a cell viability assay. As depicted in Figure 1A, the concentrations of DCY51^T-AuNps aqueous suspensions ranged from 0.1 to 100 μg mL^{-1}. The intracellular reactive oxygen species (ROS) levels in response to lipopolysaccharide (LPS) were markedly elevated compared to unstimulated cells. Additionally, concentrations of DCY51^T-AuNps aqueous suspensions exceeding 10 μg mL^{-1} demonstrated significant inhibition of intracellular ROS production (Figure 1B). Past research has indicated a correlation between lipopolysaccharide (LPS)-induced intracellular reactive oxygen species (ROS) production and the activation of NF-κB. Additionally, redox-sensitive mitogen-activated protein kinases (MAPKs) like JNK have been identified in these processes (Parker et al., 2018). To investigate the potential involvement of intracellular redox states in the inhibition of NF-κB signaling by DCY51^T-AuNps aqueous suspensions, the levels of intracellular ROS production were examined. Following treatment with 10 μg mL^{-1} DCY51^T-AuNps aqueous suspensions, the intracellular ROS level was found to be even lower than in untreated cells. This outcome suggests that the suppressive effects of DCY51^T-AuNps aqueous suspensions on MAPK and NF-κB signaling are, at least in part, associated with a reduction in intracellular ROS (Li et al., 2023).

Impact of DCY51^T-AuNps Aqueous Suspensions on NO and PGE2 Production in RAW264.7 Cells

The introduction of LPS (1 μg mL^{-1}) resulted in an elevation in nitrite production compared to RAW264.7 cells not treated with LPS, as illustrated in Figure 2A. The assessment of nitrite production through Griess reagent assay revealed that DCY51^T-AuNps aqueous suspensions led to a reduction in NO production when compared to cells treated with LPS. Cells treated with DCY51^T-AuNps aqueous suspensions at a concentration of 10 μg mL^{-1} exhibited a similar level to the positive control (1 μM Dexamethasone). Additionally, qRT-PCR and western blot analyses (Figure 2E and F) demonstrated a decrease in the expression of inducible nitric oxide synthase (iNOS) in LPS-induced RAW264.7 cells treated with DCY51^T-AuNps aqueous suspensions. Various concentrations of DCY51^T-AuNps aqueous suspensions were observed to reduce LPS-induced PGE2 release (Figure 2B). Furthermore, DCY51^T-AuNps aqueous suspensions exhibited a notable impact on the mRNA and protein levels of cyclooxygenase-2 (COX-2) in LPS-stimulated RAW264.7 cells (Figure 2C and D).

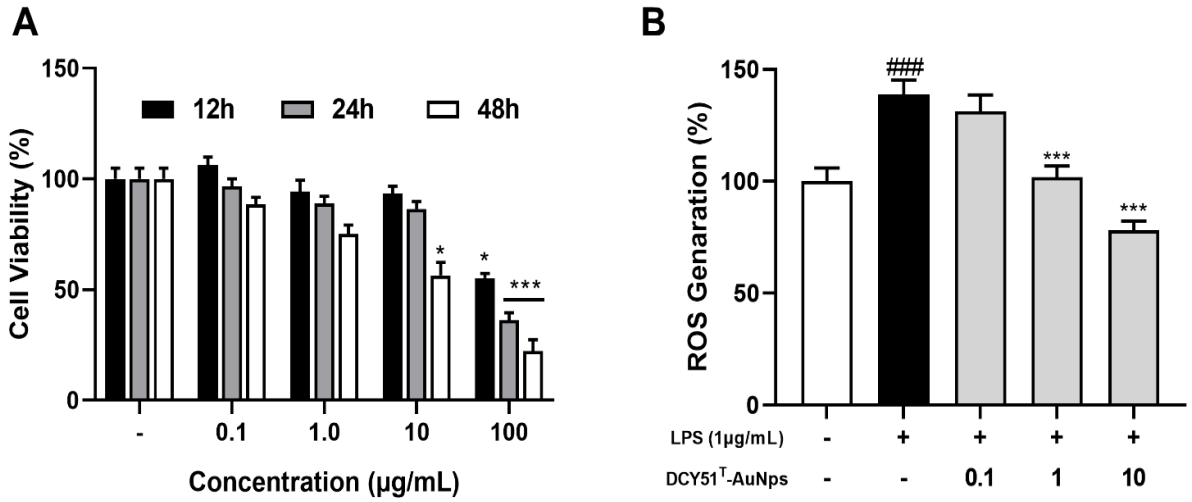

Figure 1. Effect of DCY51^T-AuNps aqueous suspensions on cell viability (A) and intracellular ROS (B) of RAW264.7 cells at different concentrations. The presented values represent the mean ± standard deviation from three separate experiments. The notation ### signifies a significance level of $p < 0.001$ compared to control cells, while * denotes $p < 0.05$, ** denotes $p < 0.01$, and *** denotes $p < 0.001$ in comparison to LPS-treated cells, respectively.

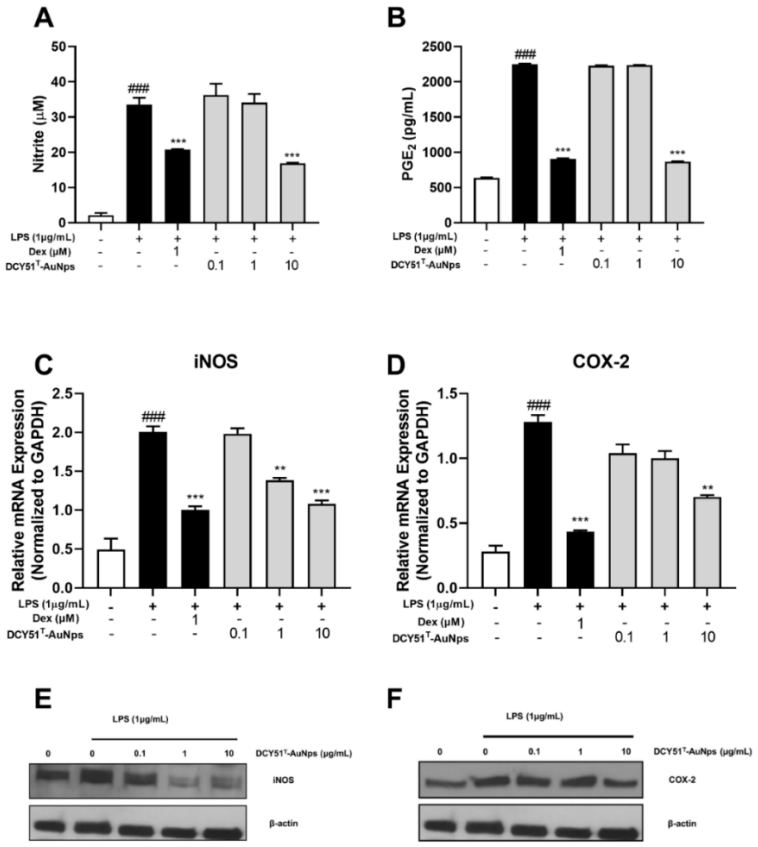

Figure 2. Nitrite production (A) and PGE2 production (B) were assessed in the culture medium of RAW264.7 cells subjected to either LPS stimulation (1 μg mL^{-1}) or left untreated, followed by treatment with varying concentrations of $DCY51^T$-AuNps aqueous suspensions (0.1, 1, and 10 μg mL^{-1}) for 24 hours. Dexamethasone (1 μM) served as a positive control. The evaluation included iNOS mRNA expression (C), iNOS protein levels (E), COX-2 mRNA expression (D), and protein levels (F). Both the mRNA expression data and Western blot data were normalized to β-actin expression. The presented values represent the mean ± SD from three independent experiments. The notation ### denotes a significance level of $p < 0.001$ compared to control cells; * indicates $p < 0.05$, ** indicates $p < 0.01$, and *** indicates $p < 0.001$ compared to LPS-treated cells, respectively.

The production of nitric oxide (NO) and prostaglandin E2 (PGE2) plays a crucial role in inflammation and immunity (Nussler & Billiar, 1993; Tomita et al., 2011). $DCY51^T$-AuNps aqueous suspension demonstrated a dose-dependent inhibition of LPS-induced NO production. In the presence of LPS (1 μg mL^{-1}), there was an elevation in nitrite production compared to RAW264.7 cells not treated with LPS. The Griess reagent assay revealed a reduction in NO production when cells were treated with $DCY51^T$-AuNps aqueous suspensions compared to LPS-treated cells. At a concentration of 10 μg mL^{-1}, the cells treated with $DCY51^T$-AuNps aqueous suspensions exhibited a level similar to the positive control, indicating a modulation of LPS-induced iNOS expression in RAW264.7 cells, consistent with a prior report (Abdul et al., 2018). Furthermore, the investigation of PGE2 activity in LPS-induced RAW264.7 cells treated with varying concentrations of $DCY51^T$-AuNps aqueous suspensions showed a dose-dependent decrease in LPS-induced PGE2 release. Additionally, the treatment of $DCY51^T$-AuNps aqueous suspensions to LPS-stimulated RAW264.7 cells had a notable impact on both mRNA and protein levels of COX-2 (cyclooxygenase) (Huang et al., 2022; Jeong & Jeong, 2010). The results unequivocally demonstrated that $DCY51^T$-AuNps aqueous suspensions strongly inhibited the activities of iNOS and COX-2.

Effects of $DCY51^T$-AuNps aqueous suspensions on the LPS-induced pro-inflammatory cytokines in RAW264.7 cells

As depicted in Figure 3A, the presence of $DCY51^T$-AuNps aqueous suspensions resulted in a significant, dose-dependent inhibition of TNF-α. A similar trend was observed in the production of

IL-6 at various concentrations of DCY51^T-AuNps aqueous suspensions (Figure 3B). Our findings unequivocally demonstrate that DCY51^T-AuNps aqueous suspensions effectively suppressed the LPS-induced pro-inflammatory cytokines in RAW264.7 cells. The qRT-PCR analysis (Figure 3C and D) further confirmed the downregulation of TNF-α and IL-6 expressions in LPS-induced RAW264.7 cells. To assess the ability of DCY51^T-AuNps aqueous suspensions to inhibit inflammatory mediators, we measured the concentrations of TNF-α and IL-6 in the culture medium of RAW264.7 cells using ELISA. The dose-dependent inhibition of TNF-α by DCY51^T-AuNps aqueous suspensions was significant, confirming their suppressive effect on LPS-induced pro-inflammatory cytokines in RAW264.7 cells (Wang et al., 2020). The qRT-PCR analysis demonstrated a reduction in the expressions of TNF-α and IL-6 in LPS-induced RAW264.7 cells, consistent with a prior study (de Araújo Júnior et al., 2016).

Suppressive Effects of DCY51^T-AuNps Aqueous Suspensions on LPS-Induced NF-κB/MAPK Activation in RAW264.7 Cells

As depicted in Figure 4, stimulation of RAW264.7 cells with LPS resulted in the activation of NF-κB, ERK, and JNK compared to untreated cells. However, DCY51^T-AuNps aqueous suspensions distinctly restrained the expression of NF-κB and the phosphorylation of ERK and JNK in comparison to levels observed in LPS-treated RAW264.7 cells. Immunofluorescence staining in Figure 5 further illustrated that exposure to LPS significantly intensified the density of NF-κB (green fluorescence), but the co-treatment with DCY51^T-AuNps aqueous suspensions significantly impeded LPS-induced nuclear translocation. The quantities of nuclear NF-κB p50 increased following LPS exposure, and this LPS-induced nuclear translocation was significantly hindered by DCY51^T-AuNps aqueous suspensions.

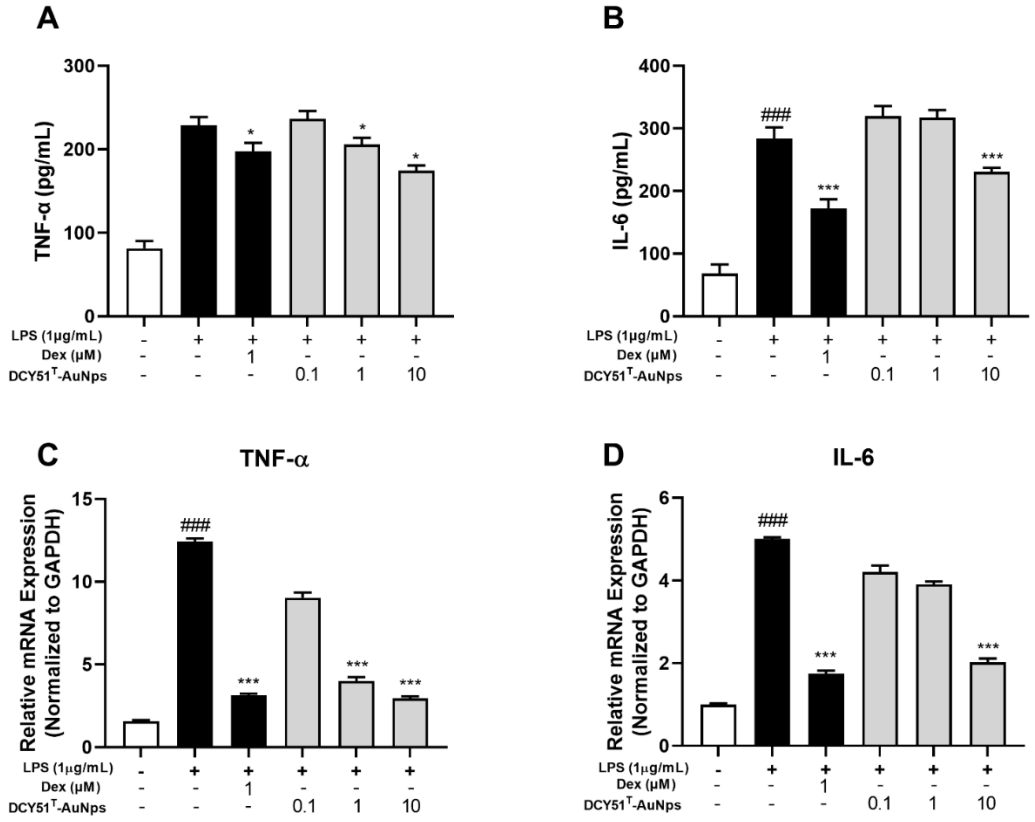

Figure 3. An evaluation was carried out on the production of TNF-α (A), IL-6 (B), TNF-α mRNA expression (C), and IL-6 mRNA expression (D). A positive control was provided by 1 μM of dexamethasone. The levels of mRNA expression were calibrated against β-actin. The values displayed are the average ± standard deviation from three separate studies. *, **, and *** show $p < 0.05$, $p < 0.01$, and $p < 0.001$ compared to LPS-treated cells, respectively. The notation ### indicates a significance level of $p < 0.001$ compared to control cells.

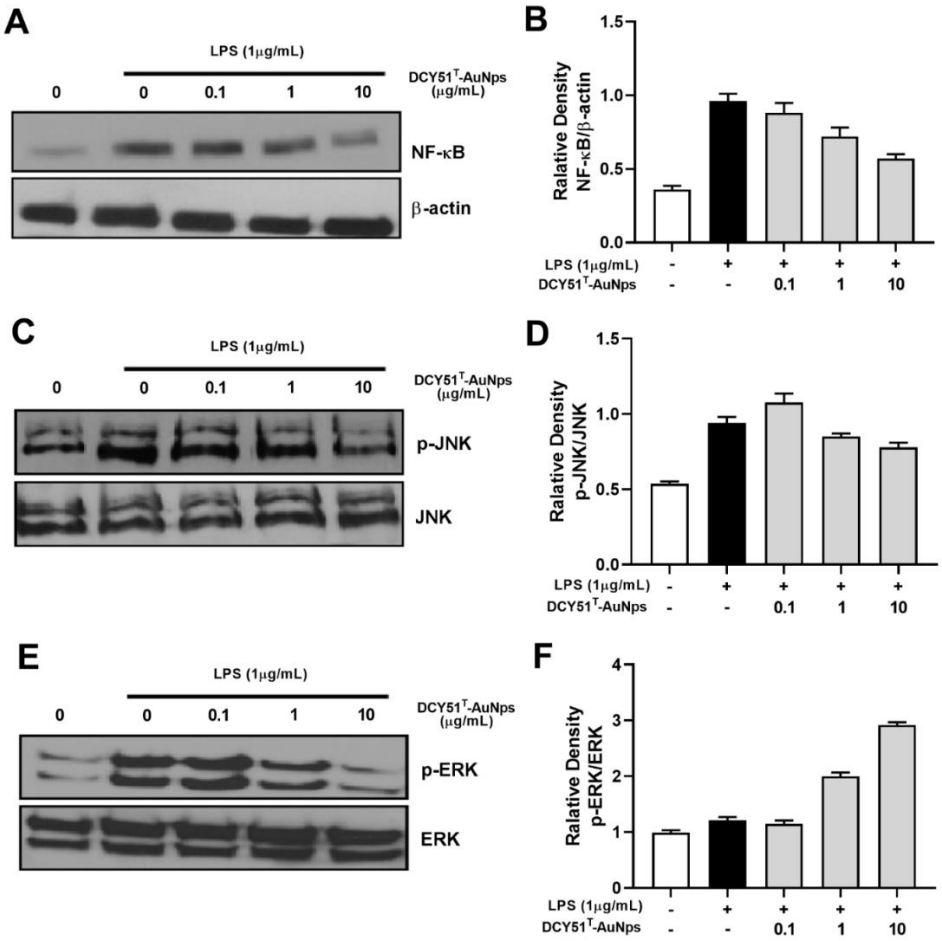

Figure 4. Assessment of the impact of DCY51^T-AuNps aqueous suspensions on NF-κB/MAPK activation. RAW264.7 cells were co-treated with various concentrations of DCY51^T-AuNps aqueous suspensions, with and without LPS (1 μg mL^{-1}). Western blot analysis of NF-κB protein expression (A) and the corresponding band density (B) are presented. The phosphorylated expression of the JNK protein level was visualized through Western blot (C), and the associated band density is depicted in (D). Protein expression levels of phospho-ERK and ERK were examined via Western blot (E). The results of Western blot band density analysis were conducted using Image J software (F). The presented values represent the mean ± SD from three independent experiments. The notation ### signifies $p < 0.001$ compared to control cells, while * indicates $p < 0.05$, ** indicates $p < 0.01$, and *** indicates $p < 0.001$ compared to LPS-treated cells, respectively.

Earlier studies have indicated a connection between the gene expression of cytokines and NF-κB through the MAPK pathway, which serves as a crucial signaling pathway in various inflammatory diseases (Feng et al., 2011; Jeong & Jeong, 2010; T. Wang et al., 2014). In light of this, we investigated the impact of DCY51^T-AuNps aqueous suspensions on the NF-κB/MAPK pathway using Western blot analysis. When RAW264.7 cells were stimulated with LPS, there was an induction of NF-κB, ERK, and JNK activation compared to untreated cells. However, DCY51^T-AuNps aqueous suspensions notably inhibited the expression of NF-κB, as well as the phosphorylation of ERK and JNK, in comparison to levels observed in LPS-treated RAW264.7 cells, consistent with prior reports (Ahn et al., 2016; Huang et al., 2022). Immunofluorescence staining in Figure 5 further revealed a distinctive enhancement in NF-κB density (green fluorescence) following LPS exposure. However, the co-treatment with DCY51^T-AuNps aqueous suspensions significantly inhibited LPS-induced nuclear translocation. Following LPS exposure, there was an increase in the quantities of nuclear NF-κB p50, and this LPS-induced nuclear translocation was significantly hindered by DCY51^T-AuNps aqueous suspensions (Sani et al., 2021).

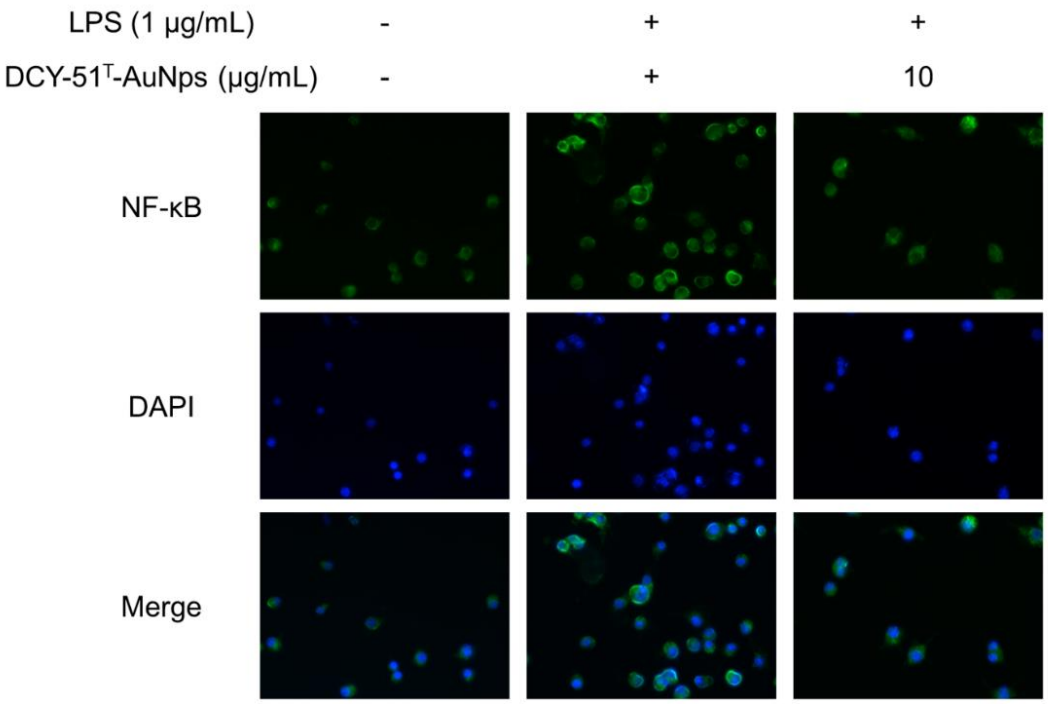

Figure 5. DCY51^{T}-AuNps aqueous suspensions suppressed the nuclear translocation of NF-κB induced by LPS in RAW 264.7 cells.

The novelty of this research is underscored by its exploration of gold nanoparticles derived from a probiotic source for biomedical applications. Specifically, the use of *Lactobacillus kimchicus* DCY51^{T} sets this study apart, emphasizing a unique approach to nanoparticle synthesis. The research reveals that these DCY51^{T}-AuNps exhibit both significant antioxidant capabilities and a low irritant effect on RAW264.7 macrophages. This novel synthesis method opens up possibilities for innovative therapeutic interventions, contributing to advancements in the field of nanomedicine. Beyond the laboratory setting, the findings of this research hold profound implications for society. The potential of DCY51^{T}-AuNps as a novel therapeutic agent for inflammation signifies a step forward in developing more effective and targeted treatments for inflammatory conditions. The innovative use of probiotic-derived nanoparticles introduces a sustainable and biocompatible approach, aligning with the growing demand for environmentally friendly medical solutions. Furthermore, the anti-inflammatory effects demonstrated by DCY51^{T}-AuNps present a promising avenue for addressing health challenges associated with inflammation, impacting the quality of life for individuals suffering from related conditions. The translational potential of this research suggests that, in the future, these nanoparticles could contribute to the development of advanced therapies with reduced side effects, thus enhancing overall healthcare outcomes for society. As such, the societal impact of this research extends to improved healthcare strategies and potential advancements in the broader field of nanomedicine.

Addressing this limitation would involve considering additional cell lines or animal models to validate and extrapolate the observed effects. Additionally, in vivo studies involving animal models could bridge the gap between in vitro findings and potential clinical applications. While our study provides valuable insights into the anti-inflammatory properties of DCY51^{T}-AuNps, the specific mechanisms underlying their action remain incompletely understood.

The novelty lies in using a probiotic-derived synthesis method, offering a sustainable and biocompatible approach to nanoparticle production. The benefit of this research not only underscores the anti-inflammatory prowess of DCY51T-AuNps on RAW264.7 macrophages but also contributes to the broader scientific discourse on the biomedical applications of gold nanoparticles synthesized from probiotic sources, potentially benefiting the development of new anti-inflammatory therapies and advancing nanomedicine.

CONCLUSION

The conclusion is, that the treatment of RAW264.7 cells with DCY51^T-AuNps aqueous suspensions inhibited LPS-induced inflammatory mediators by suppressing the protein and mRNA expression of iNOS and COX-2. DCY51^T-AuNps aqueous suspensions also decreased the mRNA expression of IL-6 and TNF-α in LPS-stimulated RAW264.7 cells. These effects are revealed by the blockage of NF-κB activation and the phosphorylation of ERK and JNK. This study successfully explored the potential of DCY51^T-AuNps in modulating inflammatory responses in RAW264.7 macrophage cells, thereby achieving the research objective.

In addition to highlighting the promising therapeutic potential of DCY51^T-AuNps, it is imperative to acknowledge the current study's limitations, providing a more nuanced perspective. One potential limitation could be the focus on a specific cell line (RAW264.7) in vitro, which may not fully represent the complex in vivo environment. Future investigations could delve deeper into the intracellular pathways and signaling cascades affected by DCY51^T-AuNps, offering a more detailed molecular understanding. Exploring the potential cytotoxic effects and long-term impacts on different cell types could also provide a more comprehensive safety profile, crucial for future therapeutic applications.

ACKNOWLEDGEMENT

We would like to thank the Faculty of Biotechnology and Center of Excellence for Food Products and Health Supplements for Degenerative Conditions, University of Surabaya, and Hanbang Bio Laboratory, Kyung Hee University, for all in-kind support of this research.

REFERENCES

Abdul, Q. A., Seong, S. H., Ahn, B. R., Islam, M. N., Jung, H. A., & Choi, J. S. (2018). Anti-inflammatory Potential of *Artemisia capillaris* and Its Constituents in LPS-induced RAW264.7 Cells. *Natural Product Sciences*, *24*(3), 171–180. doi: 10.20307/nps.2018.24.3.171

Agarwal, H., Nakara, A., & Shanmugam, V. K. (2019). Anti-inflammatory mechanism of various metal and metal oxide nanoparticles synthesized using plant extracts: A review. *Biomedicine & Pharmacotherapy*, *109*, 2561–2572. doi: 10.1016/j.biopha.2018.11.116

Ahn, S., Siddiqi, M. H., Aceituno, V. C., Simu, S. Y., & Yang, D. C. (2016). Suppression of MAPKs/NF-κB activation induces intestinal anti-inflammatory action of ginsenoside Rf in HT-29 and RAW264.7 cells. *Immunological Investigations*, *45*(5), 439–449. doi: 10.3109/08820139.2016.1168830

Ahn, S., Siddiqi, M. H., Aceituno, V. C., Simu, S. Y., Zhang, J., Jimenez Perez, Z. E., Kim, Y.-J., & Yang, D.-C. (2016). Ginsenoside Rg5: Rk1 attenuates TNF-α/IFN-γ-induced production of thymus-and activation-regulated chemokine (TARC/CCL17) and LPS-induced NO production via downregulation of NF-κB/p38 MAPK/STAT1 signaling in human keratinocytes and macrophages. *In Vitro Cellular & Developmental Biology-Animal*, *52*, 287–295. doi: 10.1007/s11626-015-9983-y

Ahn, S., Siddiqi, M. H., Noh, H.-Y., Kim, Y.-J., Kim, Y.-J., Jin, C.-G., & Yang, D.-C. (2015). Anti-inflammatory activity of ginsenosides in LPS-stimulated RAW 264.7 cells. *Science Bulletin*, *60*, 773–784. doi: 10.1007/s11434-015-0773-4

Ahn, S., Singh, P., Castro-Aceituno, V., Yesmin Simu, S., Kim, Y. J., Mathiyalagan, R., & Yang, D. C. (2017). Gold nanoparticles synthesized using *Panax ginseng* leaves suppress inflammatory - mediators production via blockade of NF-κB activation in macrophages. *Artificial Cells, Nanomedicine, and Biotechnology*, *45*(2), 270–276. https://doi.org/10.1080/21691401.2016.1228661

Ahn, S., Singh, P., Jang, M., Kim, Y.-J., Castro-Aceituno, V., Simu, S. Y., Kim, Y. J., & Yang, D.-C. (2018). Gold nanoflowers synthesized using *Acanthopanacis cortex* extract inhibit inflammatory mediators in LPS-induced RAW264. 7 macrophages via NF-κB and AP-1 pathways. *Colloids and Surfaces B: Biointerfaces*, *162*, 398–404. doi: /10.1016/j.colsurfb.2017.11.037

Alkilany, A. M., & Murphy, C. J. (2010). Toxicity and cellular uptake of gold nanoparticles: what we have learned so far? *Journal of Nanoparticle Research*, *12*, 2313–2333. doi: 10.1007/s11051-010-9911-8

Bansal, S. A., Kumar, V., Karimi, J., Singh, A. P., & Kumar, S. (2020). Role of gold nanoparticles in advanced biomedical

applications. *Nanoscale Advances*, *2*(9), 3764–3787. doi: 10.1039/D0NA00472C

Beinke, S., & Ley, S. C. (2004). Functions of NF-κB1 and NF-κB2 in immune cell biology. *Biochemical Journal*, *382*(2), 393–409. doi: 10.1042/BJ20040544

Fatimah, I., Hidayat, H., Nugroho, B. H., & Husein, S. (2020). Ultrasound-assisted biosynthesis of silver and gold nanoparticles using *Clitoria ternatea* flower. *South African Journal of Chemical Engineering*, *34*, 97–106. doi: 10.1016/j.sajce.2020.06.007

Feng, D., Zhou, Y., Xia, M., & Ma, J. (2011). Folic acid inhibits lipopolysaccharide-induced inflammatory response in RAW264. 7 macrophages by suppressing MAPKs and NF-κB activation. *Inflammation Research*, *60*, 817–822. doi: 10.1007/s00011-011-0337-2

Fernandes De Araújo Júnior, R., Antunes De Araújo, A., Bispo Pessoa, J., Neto, P. F., Ribeiro Da Silva, G., Luiza, A., Leitão Oliveira, C. S., Gomes De Carvalho, T., Silva, H. F. O., Eugênio, M., Sant'anna, C., & Gasparotto, L. H. S. (2016). Anti-inflammatory, analgesic and anti-tumor properties of gold nanoparticles. *Pharmacological Reports*, *69*(1), 119-129. doi: 10.1016/j.pharep.2016.09.017

Gasparini, C., & Feldmann, M. (2012). NF-κB as a target for modulating inflammatory responses. *Current Pharmaceutical Design*, *18*(35), 5735–5745. doi: 10.2174/ 138161212803530763

Hart, L. A., Krishnan, V. L., Adcock, I. M., Barnes, P. J., & Chung, K. F. (1998). Activation and localization of transcription factor, nuclear factor-κ B, in asthma. *American Journal of Respiratory and Critical Care Medicine*, *158*(5), 1585–1592. doi: 10.1164/ajrccm.158.5.9706116

Huang, P., Hong, J., Mi, J., Sun, B., Zhang, J., Li, C., & Yang, W. (2022). Polyphenols extracted from *Enteromorpha clathrata* alleviates inflammation in lipopolysaccharide-induced RAW 264.7 cells by inhibiting the MAPKs/NF-κB signaling pathways. *Journal of Ethnopharmacology*, *286*, 114897. doi: 10.1016/j.jep.2021.114897

Huq, M. A., Ashrafudoulla, M., Rahman, M. M., Balusamy, S. R., & Akter, S. (2022). Green synthesis and potential antibacterial applications of bioactive silver nanoparticles: A review. *Polymers*, *14*(4), 742. doi: 10.3390/polym14040742

Jeong, J. B., & Jeong, H. J. (2010). Rheosmin, a naturally occurring phenolic compound inhibits LPS-induced iNOS and COX-2 expression in RAW264. 7 cells by blocking NF-κB activation pathway. *Food and Chemical Toxicology*, *48*(8–9), 2148–2153. doi: 10.1016/j.fct.2010.05.020

Kyriakis, J. M., & Avruch, J. (2012). Mammalian MAPK signal transduction pathways activated by stress and inflammation: a 10-year update. *Physiological Reviews*, *92*(2), 689–737. doi: 10.1152/physrev.00028.2011

Li, K., Hu, W., Yang, Y., Wen, H., Li, W., & Wang, B. (2023). Anti-inflammation of hydrogenated isoflavones in LPS-stimulated RAW264. 7 cells via inhibition of NF-κB and MAPK signaling pathways. *Molecular Immunology*, *153*, 126–134. doi: 10.1016/j.molimm.2022.11.019

Liu, F., Sun, G., Gao, H., Li, R., Soromou, L.-W., Chen, N., Deng, Y.-H., & Feng, H. (2013). Angelicin regulates LPS-induced inflammation via inhibiting MAPK/NF-κB pathways. *Journal of Surgical Research*, *185*(1), 300–309. doi: /10.1016/j.jss.2013. 05.083

Livak, K. J., & Schmittgen, T. D. (2001). Analysis of relative gene expression data using real-time quantitative PCR and the 2− ΔΔCT method. *Methods*, *25*(4), 402–408. doi: 10.1006/meth.2001.1262

Markus, J., Mathiyalagan, R., Kim, Y.-J., Abbai, R., Singh, P., Ahn, S., Perez, Z. E. J., Hurh, J., & Yang, D. C. (2016). Intracellular synthesis of gold nanoparticles with antioxidant activity by probiotic *Lactobacillus kimchicus* DCY51^{T} isolated from Korean kimchi. *Enzyme and Microbial Technology*, *95*, 85–93. doi: 10.1016/ j.enzmictec.2016.08.018

Medzhitov, R. (2008). Origin and physiological roles of inflammation. *Nature*, *454*(7203), 428–435. doi: 10.1038/nature07201

Nussler, A. K., & Billiar, T. R. (1993). Inflammation, immunoregulation, and inducible nitric oxide synthase. *Journal of Leukocyte Biology*, *54*(2), 171–178. doi: 10.1002/jlb.54.2.171

Pan, Y., Neuss, S., Leifert, A., Fischler, M., Wen, F., Simon, U., Schmid, G., Brandau, W., & Jahnen-Dechent, W. (2007). Size-dependent cytotoxicity of gold nanoparticles. *Small*, *3*(11), 1941–1949. doi: 10.1002/smll. 200700378

Parker, L., Trewin, A., Levinger, I., Shaw, C. S., & Stepto, N. K. (2018). Exercise-intensity dependent alterations in plasma redox status do not reflect skeletal muscle redox-sensitive protein signaling. *Journal of Science and Medicine in Sport*, *21*(4), 416–421. doi: 10.1016/j.jsams.2017.06.017

Rehman, M. U., Yoshihisa, Y., Miyamoto, Y., & Shimizu, T. (2012). The anti-inflammatory effects of platinum nanoparticles on the lipopolysaccharide-induced inflammatory response in RAW 264.7 macrophages. *Inflammation Research*, *61*, 1177–1185. doi: 10.1007/s00011-012-0512-0

Rius-Pérez, S., Pérez, S., Martí-Andrés, P., Monsalve, M., & Sastre, J. (2020). Nuclear factor kappa B signaling complexes in acute inflammation. *Antioxidants & Redox Signaling*, *33*(3), 145–165. doi: 10.1089/ars.2019.7975

Sani, A., Cao, C., & Cui, D. (2021). Toxicity of gold nanoparticles (AuNPs): A review. *Biochemistry and Biophysics Reports*, *26*, 100991. doi: 10.1016/j.bbrep.2021.100991

Smale, S. T. (2010). Selective transcription in response to an inflammatory stimulus. *Cell*, *140*(6), 833–844. doi: 10.1016/j.cell.2010.01.037

Su, Y.-W., Chiou, W.-F., Chao, S.-H., Lee, M.-H., Chen, C.-C., & Tsai, Y.-C. (2011). Ligustilide prevents LPS-induced iNOS expression in RAW 264.7 macrophages by preventing ROS production and down-regulating the MAPK, NF-κB and AP-1 signaling pathways. *International Immunopharmacology*, *11*(9), 1166–1172. doi: 10.1016/j.intimp.2011.03.014

Sukweenadhi, J., Setiawan, K. I., Avanti, C., Kartini, K., Rupa, E. J., & Yang, D.-C. (2021). Scale-up of green synthesis and characterization of silver nanoparticles using ethanol extract of *Plantago major* L. leaf and its antibacterial potential. *South African Journal of Chemical Engineering*, *38*(1), 1–8. doi: 10.1016/j.sajce.2021.06.008

Tomita, Y., Rikimaru-Kaneko, A., Hashiguchi, K., & Shirotake, S. (2011). Effect of anionic and cationic n-butylcyanoacrylate nanoparticles on NO and cytokine production in Raw264.7 cells. *Immunopharmacology and Immunotoxicology*, *33*(4), 730–737. doi: 10.3109/08923973.2011.565345

Wang, G., Zhan, Q., & Wu, H. (2020). Suppression of lipopolysaccharide-induced activation of RAW 264.7 macrophages by Se-methylseleno-l-cysteine. *International Immunopharmacology*, *89*, 107040. doi: 10.1016/j.intimp.2020.107040

Wang, T., Wu, F., Jin, Z., Zhai, Z., Wang, Y., Tu, B., Yan, W., & Tang, T. (2014). Plumbagin inhibits LPS-induced inflammation through the inactivation of the nuclear factor-kappa B and mitogen activated protein kinase signaling pathways in RAW 264.7 cells. *Food and Chemical Toxicology*, *64*, 177–183. doi: 10.1016/j.fct.2013.11.027

Wu, H., Wang, Y., Zhang, Y., Xu, F., Chen, J., Duan, L., Zhang, T., Wang, J., & Zhang, F. (2020). Breaking the vicious loop between inflammation, oxidative stress and coagulation, a novel anti-thrombus insight of nattokinase by inhibiting LPS-induced inflammation and oxidative stress. *Redox Biology*, *32*, 101500. doi: 10.1016/j.redox.2020.101500

Yang, S., Sharrocks, A. D., & Whitmarsh, A. J. (2013). MAP kinase signalling cascades and transcriptional regulation. *Gene*, *513*(1), 1–13. doi: 10.1016/j.gene.2012.10.033